Application of Thermography for Non-Invasive Diagnosis of Thyroid Gland Disease

Ahdy Helmy, Michael Holdmann, and Maher Rizkalla*, *Senior Member, IEEE*

***Abstract*—In this paper, a computer-based prototype device was designed based on an economical noninvasive system that could detect and display the relative skin temperature variations present in human patients suffering from thyroid disorders. Such a system could be used to augment the normal procedures followed by the physician in diagnosing the thyroid to detect areas of hyperactivity within the gland. Because a hyperactive nodule is a center of increased blood flow and chemical activity, it might be also a center of heat production that is detectable by thermal sensing. This paper also presents a finite-element analysis (FEA) of a hot thyroid nodule that is used for investigating the temperature distribution in conjunction with the prototype. The instrumentation model built was based on actual dimensional human model for thyroid nodules obtained from various patients. A software program was written in Visual Basic to detect the temperature distribution around the hot spot. The software also incorporates means to minimize the thermal noise associated with the body temperature. The FEA utilizes the same boundary values used in the practical settings. This includes initial values of temperatures for the hot spot and its surroundings. The results of the finite-element simulation assisted in the selection of the solid state sensors that were used in the instrumentation of the thermographic system. The selected sensors were calibrated for their functionality and dynamic performance according to the specifications. The new noninvasive diagnostic technique was applied to patients having Graves' diseases at the Indiana University (IU) Hospital, and compared with the existing scheme that utilizes I Scan. The results of the new diagnostic method were in good agreement with the current existing method.**

***Index Terms*—Diagnosis, finite-element analysis (FEA), infrared sensors, instrumentation, noninvasive, thermography, thyroid gland.**

I. Introduction

THERMAL imaging has been applied in many fields in medicine, including wound care [1], sport medicine [2], forensic medicine [3], anaesthesiology [4], peripheral vascular diseases [5], cancer diagnosis [6], and breast diseases [7]. So far thermography has not been utilized for nodular thyroid disease features to quantitatively measure spatial and temporal abnormalities in blood perfusion of the skin.

The issues related to thyroid gland disorders have been crucial in particular to pregnant women. More than a third of all women will be found to have at least one thyroid nodule disorder during their lifetime. In fact 12 000 cases of thyroid cancer are diagnosed annually in the U.S. The criteria by which patients with dysfunctional thyroid nodules are selected for surgical treatment are far from certain. Removal of the thyroid gland for diagnosis of a nodule has never been a satisfactory option. The risk involved in pregnant women from the use of nuclear medicine is of great concern. This is due to the radiation risk that may cross the placenta and affects the thyroid of the fetus. A safe and cost-effective prescreening method would be an advantageous over the existing Iodine-based schemes.

Because a hyperactive nodule is a center of increased blood flow and chemical activity, it might also be a center of heat production that is detectable by thermal sensing. In addition, toxic autonomous nodules tend to be large (> 2.5 cm) and this may favor the possibility of detection. However, at the present time thermography is not generally applied in this instance. This may be due to the high cost of thermal cameras or the choice of proper solid-state sensors used with a data acquisition. If another method of thermal sensing could be proven useful, it may provide the basis for more widespread diagnostic application. One possible solution would be to utilize readily available components and subsystems for a noninvasive, safe, and cost-effective prototype. In order to design a system capable of detecting and mapping temperature distribution on the surface of the skin, the limits of detector resolution must be determined. This will have a bearing on both the type of sensor and the data acquisition system chosen.

The analysis first needs to determine how much heat energy is generated by a "normal" human and then how much extra energy would be generated by a hyperactive thyroid gland or nodule. This is the purpose of the thermal analysis used in this study. By determining the limits of this quantity, a model that will enable the determination of the incremental temperature difference (between a tumor nodule and the surrounding tissue underneath the skin) at the surface of the skin, is necessary.

Section II provides data received from an existing IR camera used in comparison with the proposed system. Section III provides a description and analysis of the finite-element analysis (FEA) model of a hyperactive thyroid gland. Section IV provides the results of the FEA simulations carried out based on the model described in Section III. In Section V, a description of the prototype is given, and then the results of the study carried out on actual patients and conclusion is presented. The proposed

Manuscript received March 30, 2007. *Asterisk indicates corresponding author.*

A. Helmy is with the VA Hospital, Indianapolis, IN 46202 USA.

M. Holdmann is with the Department of Electrical and Computer Engineering, Purdue School of Engineering and Technology, Indiana University Purdue, University Indianapolis, Indianapolis, IN 46202-5137 USA.

*M. Rizkalla is with the Department of Electrical and Computer Engineering, Purdue School of Engineering and Technology, Indiana University Purdue, University Indianapolis, 723 W Michigan Street, Indianapolis, IN 46202-5137 USA (e-mail: mrizkall@iupui.edu).

Color versions of one or more of the figures in this paper are available online at http://ieeexplore.ieee.org.

Digital Object Identifier 10.1109/TBME.2008.915731

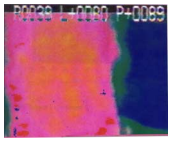

Fig. 1. Close up of the thermogram obtained for a subject via the IR camera.

Fig. 2. Control subject via INSIGHT starsight IR camera.

future work to improve the system resolution and advance it to the second stage is given with the conclusion of this paper.

II. Available Thermographic Camera System

Figs. 1 and 2 show the results of scanning the neck of a volunteer patient with thyroid problems. Each subject was preconditioned with a cold pack on the neck for 5 min. A series of sequential scans, which spanned a total of 4 min, were obtained for each subject. The two-lobed structure of the gland was apparent.

Fig. 1 shows a close up view of the thermogram obtained via the IR camera for one of the subjects used in our experiments. Typically such cameras have high spatial resolution and their normal cost near $36 000.

The noise generated from various colors is disturbing these images. Overall, the quality of these images is not acceptable for medical diagnosis, and a different sophisticated approach is required to get the temperature distribution around the hot spot. The proposed IR scanner would require an interface design of high resolution sensors with the data acquisition.

III. Proposed Model

In order to come up with a model that is simple enough to be implemented but not overly simplistic, several assumptions were made. The heating and cooling effects of blood flow in the capillaries were neglected, as was the interface between the thyroid and the inside surface of the skin. Since these assumptions would simplify the model to a hot spot under the skin surface, the model was modified to a 30 mm × 30 mm piece of skin with 10 mm embedded diameter hot nodule.

For analysis purposes, the model was subdivided into incremental cubes of total 294 nodes that fit the modeling space of the FEA software used in this paper. For the nodal loading conditions, the outside of the skin surface, which was composed of 49 nodes, was held at 29 °C, while the inside skin surface, which was also composed of 49 nodes, was held at 37 °C. The nodule (tumor) was composed of 27 nodes and its temperature varied in successive iterations.

At steady state the heat lost to the environment must balance heat produced by the human body. This heat loss, which occurs via radiation, evaporation, convection, and conduction, is necessary otherwise a fever would result. An estimate of the temperature rise that would occur in the body if no heat were lost can be derived using the specific heat of the body. This is given by [8] $dT/dt = q/mc_p$, where T is the temperature measured in Celsius, q is the heat flux, m is the mass, and c_p is the specific heat. An average 150 lb resting male, having on average a heat flux of 72 Kcal/hr and 0.86 Kcal/Kg°C specific heat [9], would experience on average a 1.2 °C rise in his body temperature per hour if no heat loss occurred.

For relatively small temperature differences, a linearized radiation film coefficient was specified [10] to simplify the model applied to the outside surface of the skin. The radiation component of heat exchange is also compensated for in the linearized radiation film coefficient. This represents the resistance of the heat flow at the boundary layer between a solid surface (skin) and air.

When performing the simulation, the temperature of the linearized radiation film is set at the arithmetic average of the skin surface and air temperatures $T_{\text{film}} = (T_{\text{skin}} + T_{\text{air}})/2$. The quantity of heat contained in the film is obtained by finding the convective and radiative components of heat flow. The convective component of heat flow depends on the Grashof (Gr), Prandtl (Pr), and Nusselt (NU) numbers [11]. These are obtained as follows: $Gr = g\beta\,(T_{\text{skin}} - T_{\text{air}})\,L^3/v^2$, where g is the acceleration due to gravity (9.8 m/s^2), $\beta = 1/T_{\text{film}}$ is the coefficient of bulk expansion, T_{film} is the film temperature in Kelvin, L the length of the film in meters, and $v = 15.68 \times 10^{-6}$ m/s is the kinematic viscosity. The Prandtl number Pr ~0.7 in the case of air, and $Nu \approx 0.59(\text{Gr}\,\text{Pr})^{0.25}$. Using $h_{\text{conv}} = kNu/L$, where $k = 0.026$ W/m°C for air, the convective component of heat flow h_{conv} can be obtained. The radiative component which is a function of the radiative constant $\sigma = 5.7 \times 10^{-8}$ W/m^2°K [12] and temperature differences is given by $h_{\text{rad}} = \sigma\left(T_{\text{skin}}^4 - T_{\text{air}}^4\right)/T_{\text{skin}} - T_{\text{air}}$. The total heat quantity in the film is $h_{\text{total}} = h_{\text{conv}} + h_{\text{rad}}$. Finally, the nodular diameter was set at 10 mm and its depth below the kin surface set at 5 mm.

IV. Simulations

The purpose of this simulation was to determine the resolution of the temperature distribution that may lead to the selection of the infrared sensors used in the design. In the simulations, a baseline in which the nodule was absent was initially considered. This was done to determine the volumetric heat generation rate that keeps the skin surface temperature at 29 °C. In this case, only the convective surface conditions and the heat generation rate were specified. The heat generation rate q' is given by $q' = Q'/V$, where V is the skin volume and Q' is the total heat lost. Q' is given by $Q' = A \times \left(1.85 \times 10^{-5}\,(\text{W/mm}^2\text{C})\right)(T_{\text{skin}} - T_{\text{air}})$, where A is the skin surface area. These parameters were utilized in the simulation, which was repeated a number of times to determine the minimum temperature differential needed on one side of the skin to observe a minimum of a 0.1 degree differential on the skin surface.

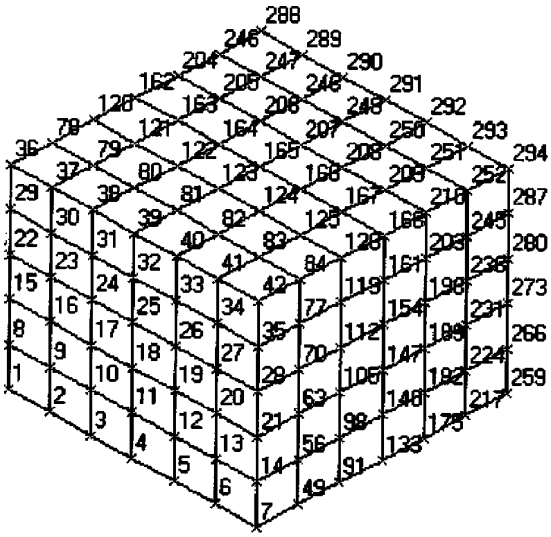

Fig. 3. Finite-element grid used for computer simulation.

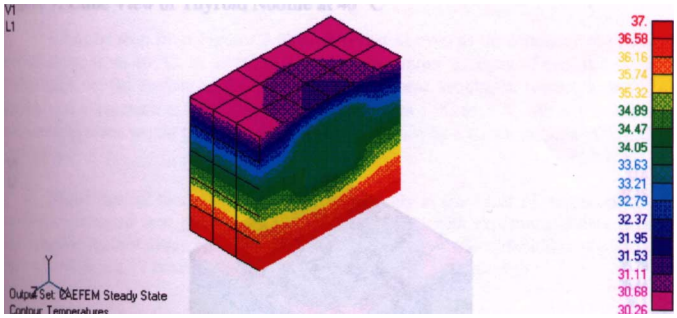

Fig. 4. Sliced view of thyroid nodule at 34 °C.

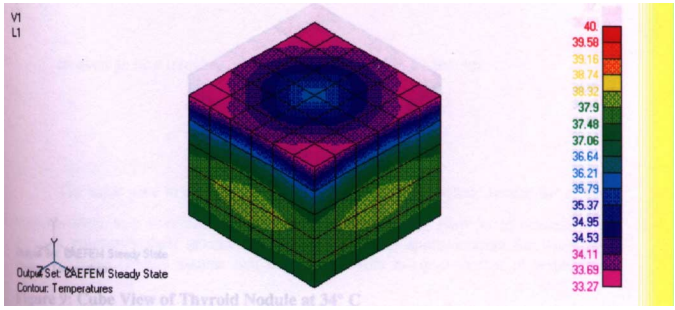

Fig. 5. Cube view of thyroid nodule at 40 °C.

Figs. 4 –7 demonstrate that even though the temperature of the nodule drops from 40 °C to 34°C, a temperature gradient of almost 1 °C is still evident on the surface of the skin. Based on these results it would appear that a hyperactive toxic thyroid nodule that was 1 °C to 3 °C warmer than its surrounding tissue, would be detectable at the skin surface by a sensor capable of 0.5 °C resolutions.

In the previous simulation (see Figs. 3–6), an initial temperature was used. In practice, this is done by cooling off the human neck to minimize the thermal noise associated with the body noise. Approximately, an initial temperature around 34 °C was considered and tested. As it can be seen, a resolution of the order of 0.1 °C may be required for the temperature detection.

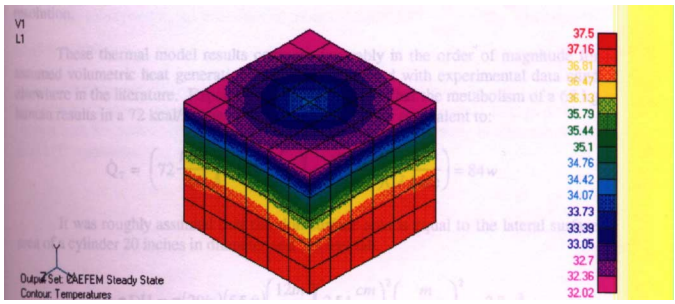

Fig. 6. Cube view of thyroid nodule at 37 °C.

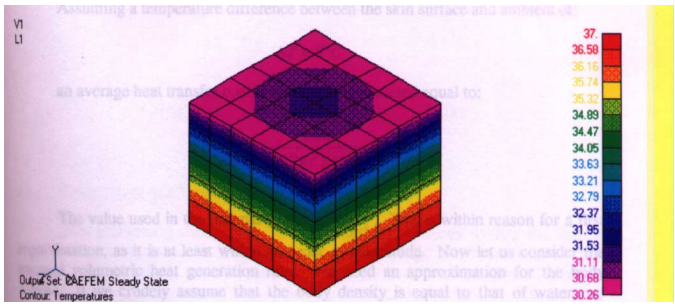

Fig. 7. Cube view of thyroid nodule at 34 °C.

V. Prototype Construction

In order to map the temperature distribution of the neck, several types of temperature transducers were considered for use. These included contact thermocouples, non-contact infrared thermocouples, resistance temperature detectors (RTDs), thermistors, and liquid crystal sensors. The sensor chosen was the non-contact infrared (IR) thermocouple for its wide temperature range, simplicity, and durability. In addition, it has the capability of sensing the temperature of the skin at a distance. Having chosen the sensor, the data acquisition (DAQ) system was then chosen. The criteria governing the choice of the DAQ system were resolution, cost per channel, and the programming environment. The system chosen was a Sensoray 518 card, which has a 16-bit resolution on eight differential-input channels, a cold-junction compensation circuit, and a 0.1 °C thermocouple temperature resolution. The combination of the IR thermocouple and DAQ board were then tested to verify that they would function together and produce a readable data file.

In order to scan the entire gland using the sensors, the MD-2 system by Arricks Robotics, which includes stepper motors, was chosen. A prototype system was then built and tested. This consisted of a linear array of eight IR sensors that were mounted 1.5 cm apart, a housing unit made of plywood covered with vinyl for protection, a chin rest, and the motion control system.

VI. Appropriate Solid State Sensors for Thermography

A. Sensing Materials

In this paper, the possibility of manufacturing continuous sensor arrays suitable to scan a human neck was considered. Various semiconductor and metal materials that are capable to sense temperature change within a human neck were considered from their sensitivities and appropriateness to be interfaced

TABLE I
VARIOUS SOLID-STATE SENSORS USED FOR TEMPERATURE DETECTIONS

Device	Thermocouple	RTD	Thermistor	Liquid Crystal Sensor
Measured Parameter	Voltage	Resistance	Resistance	Color change
Advantages	• Simplicity • Durability • Low cost • Self-Powered • Wide variety • Wide temperature range	• Accuracy • Stability • More linear than thermo-couple	• Fast response time • High output • 2-wire Ohms measure-ment • Very sensitive	• Simplicity • Durability
Disadvantages	• Non-Linearity • Low voltage signal • Requires reference • Least stable • Least sensitive	• High cost • Self-Heating • Requires current source • Small output signal • Low absolute resistance	• Non-Linearity • Limited temperature range • Self-Heating • Requires current source • Fragile	• Limited temperature range • Slow response time • Limited configur-ations

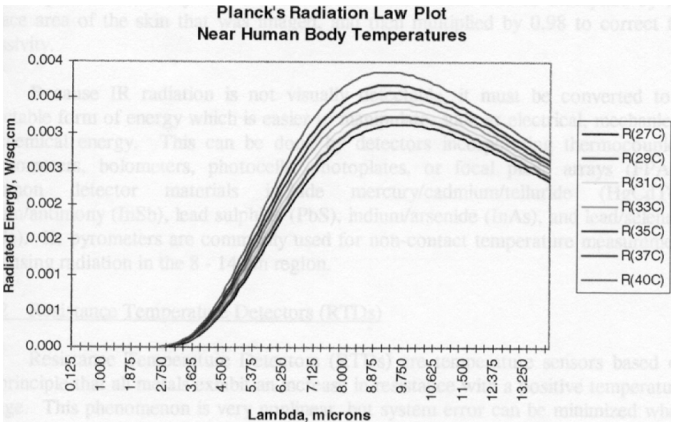

Fig. 8. Planck's law of radiant energy plotted for biomedical temperatures.

with data acquisition system. Various materials such as Mercury/cadmium/telluride (HgCdTe), Indium/antimony (InSb), Indium/arsenide (InAs), and Lead selenate (PbSe), were studied with respect to their temperature range, resolution, sensitivity, and interfacing to computer peripherals and application to human. Fig. 8 gives the spectral Planck's radiation for the power spectral near 37 °C. As it can be seen, the wavelength between 6 to 12 μm is required to maximum power efficiency. This information is incorporated in the selection of the IR sensors applied to the design of the instrumentation.

The problems associated with these materials when used as a distributed IR sensor includes difficulty with measuring emf generated from different spots and the measuring resistance reflecting the temperature change across the surface of the human neck. This suggested that discrete sensors must be used to get temperature distribution around the hot spot of the gland nodule.

B. Discrete Sensors

Table I gives a summary of all possible infra red detectors that exist in the market with their advantages and disadvantages as applied to human temperatures.

1) Elaboration on the IR Devices:

Thermistors: These are characterized by the following:

- widely used in medical filed because of their sensitivity in the desired temperature range;
- resistance with high temperature coefficients.

Thermocouples:

- contact and non-contact (passive);
- seebeck effect for two dissimilar metal junctions (emf that raises current);
- J-type junctions are suitable for human skin application for both contact and non-contact sensors;
- linear within 25 °C to 45 °C;
- 5 μV per 0.1 °C change.

For 16 bit A/D over 1.25 V, resolution near 19 μV that correspond to 0.4 °C can be achieved. If the input is amplified by a factor of 10, a sensitivity of 0.1 °C is attainable.

Problems associated with direct contact sensors include the following:

- not good thermal contact;
- heat dissipated by the sensor causes rise of temperature;
- the ambient temperature may change the sensor temperature is no zero thermal conductance between the sensor and object;
- the mass of the sensor must be small enough so as not to significantly alter the temperature of the object being measured.

Therefore, non-contact sensors are advantageous for this application.

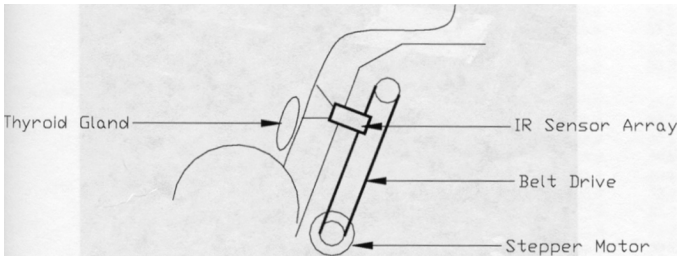

Fig. 9. Setup of the structure of the IR sensor, stepper motor, and drive.

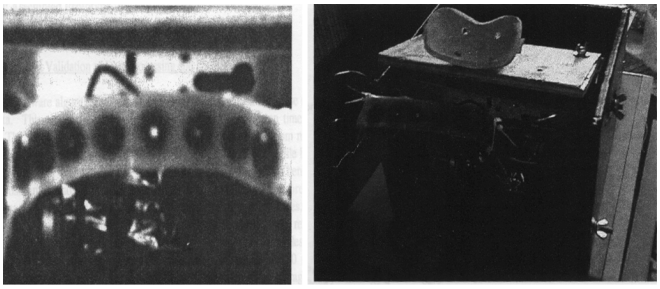

(a) (b)

Fig. 10. Sensor array in the left-hand side (a) and the instrumentation on the right-hand side (b).

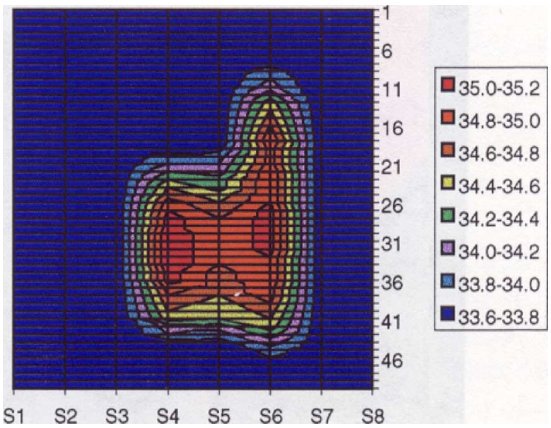

Fig. 11. Thermogam of control subject with Graves Disease-sequence B.

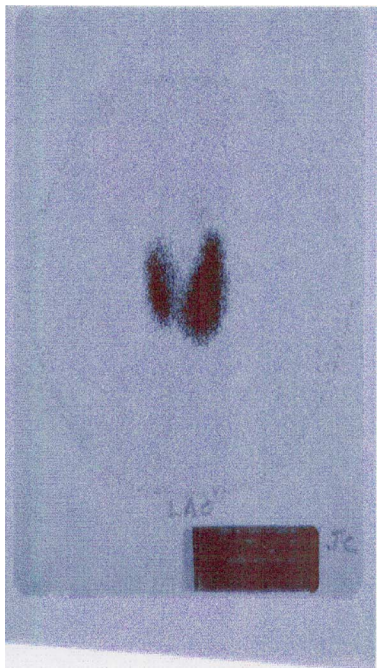

Fig. 12. ^{123}I scan for a patient with Graves Disease-ANT view.

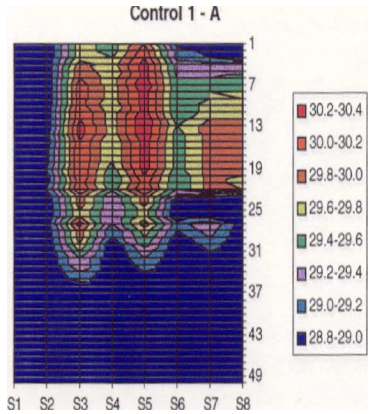

Fig. 13. Patient scan for multiple nodules (first attempt).

Resistive Temperature Detectors (RTD): These sensors are based on the fact that metals exhibit a resistance increase with temperature, which can be detected by a bridge circuit.

Liquid Crystal Sensors:

- contact thermography;
- they reflect light within a narrow spectrum of wave length in the visible range;
- it would produce false reading when heating and cooling the skin;
- slow response to heat variation;
- application is hard with bony areas.

According to the selection criterion, the IR thermocouple which was used has the following characteristics:

- non-contact type was chosen;
- IRt/c0.1 manufactured by Exergen Corporation, Newton, MA;
- J-type with special biomedical calibration;
- calibrated ± 0.2 °C within the range of 25 °C to 40 °C);
- spectral response of 6.5 to 14 μm;
- response time constant of 80 ms;
- \$100/each.

This was found to be the best fit in our design achieving required sensitivity, fast response, high output, linearity, cost, emissivity within human temperature range, and interfacing with data DAQ system

VII. Computer Instrumentation and Design of Probe Sensor

In this design, eight IR thermocouples (Exergen IRtc0.1) were connected to a CYDAS 1600 data acquisition card installed in PC. The card uses an ADS7805 successive approximation A/D with a conversion time of 10 μs. This is well within the range of the response time of the IR Thermocouples. The resolution based on range of 1.25 V, 16-bit resolution, was found to be 19 μV. The board was programmed with BASIC

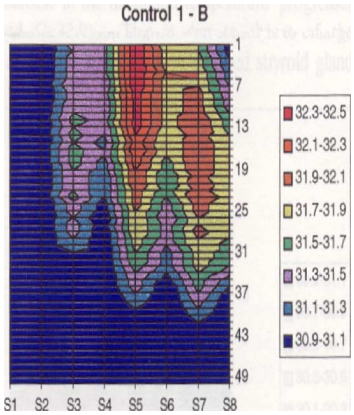

Fig. 14. Patient scan with multiple nodules (second attempt).

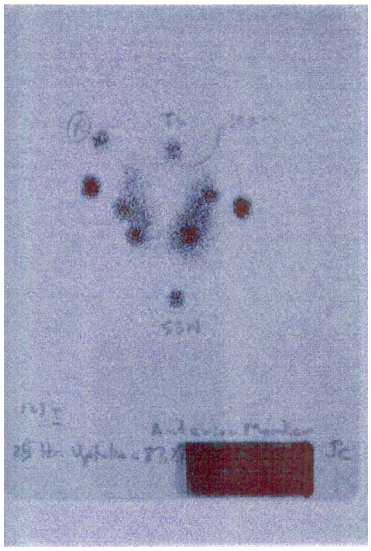

Fig. 15. Iodine scan for a patient with multiple nodules.

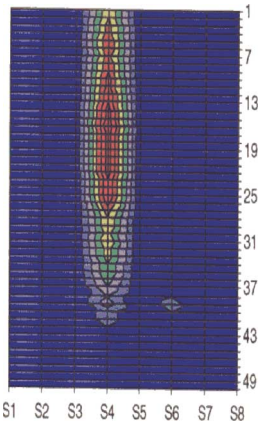

Fig. 16. Thermographic image for a patient with one nodule was detected.

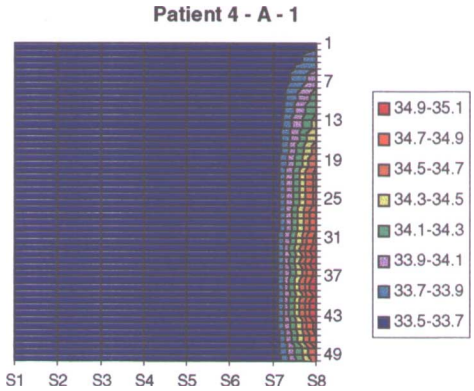

Fig. 17. Thermogam for a patient where a small portion of a nodule was detected.

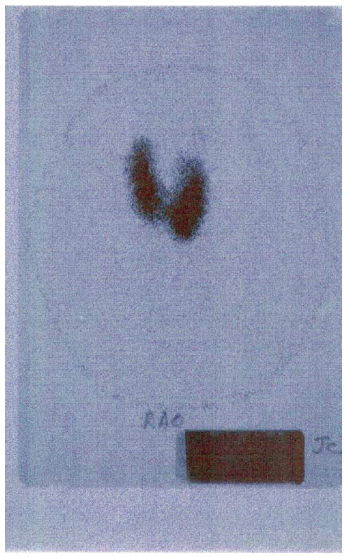

Fig. 18. Iodine scan used in the study for Figs. 15 and 16.

to scan all the eight channels once every time ENTER key was pressed.

The data reading was automatically taken at each vertical position of the sensor array and recorded into a data file. Twelve rows by eight columns make a series for five round trips for the motor system. This makes ten data readings for each sensor location. The software written in visual basic was averaging these data for minimizing thermal noise in the process. The spacing between steps was calculated by the stepper motor to cover enough area including the gland. Twelve vertical steps were taken with the eight horizontal sensor arrays. The motion control system: MD-2 system by Arrick Robotics is a dual-axis control that was appropriate for the design. Figs. 9 and 10 show the sensor array beneath the human chin position.

VIII. Results and Discussions

The study conducted in this paper has received an approval from the Institutional Review Board at the VA Hospital of Indianapolis to be applied to patients in the hospital. The following results were obtained from the new instrumentation and compared with the traditional method of diagnosis.

Fig. 12 shows the scanning results for a patient suffering from Diffuse Toxic Goiter (Graves Disease). The patient's thyroid gland has no areas of localized hyperactivity; instead the entire gland is hyperactive. Fig. 12 shows a result from having scanned the patient with ^{123}I scanning. Data presented in Figs. 13–15

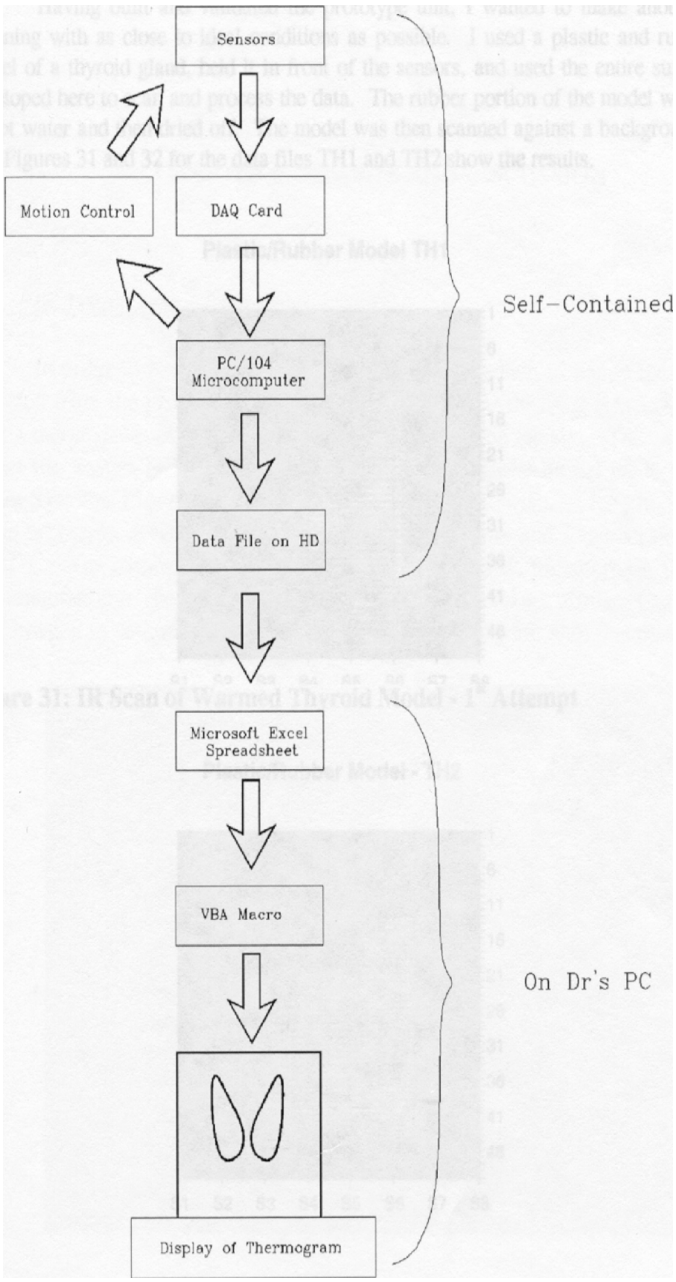

Fig. 19. Proposed future setting for the thermographic scan.

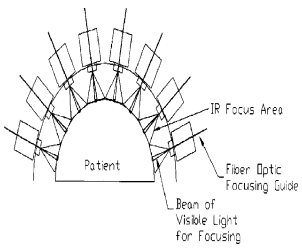

Fig. 20. Use of fiber optic focusing guide for future scan.

show two attempts for a patient with multiple nodules as compared with the Iodine scan shown in Fig. 15. In all scans, the radiation is detected with uniform density in both lobes of the thyroid. No area of localized hyperactivity was detected, but

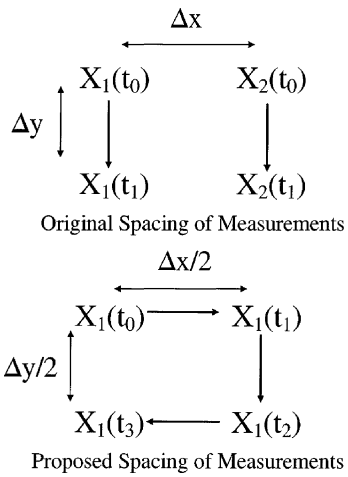

Fig. 21. X–Y sensor motion shown for one sensor.

the thyroid's ^{123}I uptake was measured at 68.1% of the amount that was ingested. Since the normal range of Iodine uptake is 10%–35%, the patient's condition was considered to be a Diffuse Toxic Goiter.

Due to the fact that discrete sensors were used, some of the hot spot locations between sensors may not be detected. This is related to the indefinite reference point of the scan and the spacing between the sensors. Fig. 16 shows one hot spot as supposed to be two close nodule spots given in Fig. 18. Fig. 17 shows one portion of a hot nodule detected by the instrumentation in another attempt for the same patient.

IX. Conclusion and Discussion

Thermography has been proposed as an alternative to more costly, invasive, or contra-indicated medical imaging methods for diagnosing thyroid abnormalities. The prototype of a modular system for noninvasive, safe, and cost-effective thyroid thermography has been proven its usefulness in data collection and processing. Finite element analysis was used to determine the required sensor resolution. The results of simulation predicted that a resolution of 0.1 °C would be adequate to solve the problem. This model was developed in order to determine the necessary resolutions for thermal sensors that will be used to obtain thermal images of patients' necks. Sensors and motion control were chosen based on their suitability and cost. The ten scans for each node on the skin surface and the time response of these sensors were found to be appropriate for the noise generated near the body temperature.

However, the preliminary data obtained with these instrumentations is far from refined, it can be concluded that the thermograms obtained roughly define the structure of the thyroid gland. There still a number of problems associated with the system. This includes variability in sensor-skin distance, optical overlap in focusing alignment, and limited resolution obtained with eight discrete sensors. A proposed methodology for future consideration that takes the system to the next level includes wireless communication link between the patient position and the doctor's office as shown in Fig. 19, and the use of fiber optics to focus the infra red area used for the scan as shown in Fig. 20. Continuous sensing area on the human neck will have a

better resolution rather than discrete sensor scanning. A future scheme to increase the number of scanned nodes is shown in Fig. 21 (demonstrated for one sensor). This is based on moving the sensors in two dimensions for half of the step distances. In this scheme, 16×16 node points will be scanned rather than the 8×8 scanned here (four times the number of nodes shown in the finite element grid in Fig. 3). The sensors' response time and data acquisition system are fast enough to handle the data received from the nodes before any significant change in the temperature takes place. This new scheme will lead to a better resolution of the thyroid images. In addition, the data processing could be managed by other software, such as LabView to either promote development as a self-contained unit, or in order to eliminate dependence on Microsoft Excel program. In addition, considering x–y scan may cover higher number of nodes in the neck area to include various nodule sizes of thyroid patients.

REFERENCES

[1] C. D. Jones, P. Plassman, E. F. J. Ring, and B. Belem, "Measurement of wound 3D shape and color (abstract)," *Imag. Sci. J.*, vol. 54, no. 1, p. 62, 2006.

[2] P. Bonnet, D. B. hare, CD Jones, E. F. J. Ring, and C. J. hare, "Preliminary observations on the effect of sports massage on the heat distribution of lower limb muscles during graded exercise tests," *Thermography Int.*, vol. 16, no. 4, pp. 143–149, 2006.

[3] K. Ammer and E. F. J. Ring, "Application of thermal imaging on forensic medicine," *Imag. Sci. J.*, vol. 53, pp. 125–131, 2005.

[4] Lawson *et al.*, "Infrared thermography in the detection and management of coronary artery disease," *Amer. J. Cardiol.*, vol. 72, pp. 894–896, 1993.

[5] J. J. Aauer *et al.*, "Hand skin blood in diabetic patients with autonomic neuropathy and microangiopathy," *Diabetes Care*, vol. 14, pp. 897–902, 1991.

[6] C. Farrell, C. Mansfield, and J. Wallace, "Thermography as an aid in the diagnosis of tumors and detection of metastatic bone disease," *Br. J. Radiol.*, vol. 44, p. 897, 1971.

[7] T. Strangi, G. Lombardi, M. P. Braccili, E. Lo-Sterzo, A. Lalli, and A. Pennesi, "Peripheral vascular hyperactivity in aterial hypertension," *Int. J. Cardiol.*, vol. 25, pp. S57–61, 1989.

[8] E. K. Chan and J. A. Pearce, "Visualization of dynamic subcutaneous vasomotor response by computer-assisted thermography," *IEEE Trans. Biomed. Eng.*, vol. 37, no. 8, pp. 786–795, Aug. 1990.

[9] J. C. Kotz and K./ F. Purcell, *Chemistry and Chemical Reactivity*. Philadelphia, PA: Saunders College, 1987.

[10] D. O. Cooney, *Biomedical Engineering Principles*. New York: Marcel-Deccer Inc., 1976, vol. 2.

[11] K. Feith, *Principles of Heat Transfer*. Scranton, PA: International Textbook Company, 1966, pp. 326–359.

[12] J. P. Holman, *Heat Transfer*. New York: McGraw-Hill, 1977, pp. 235–272.

Ahdy Helmy received the M.B.B.Ch. and the Ph.D. degrees from Alexandria University, Egypt, in 1981 and 1992, respectively.

In 1995, he joined the IU Medical School, where he is currently a Professor of Clinical Medicine with the Department of Medicine, School of Medicine, University Graduate School, Indiana University-Purdue University (IU), Indianapolis, IN. In 2001, he cofounded the Primary-Care Interdisciplinary Medical Education (PRIME) Clinic, the Richard L. Roudebush Veterans Administration Medical Center, Indianapolis. He has been widely recognized for his exceptional teaching. His research interests include noninvasive procedures as applied to endocrinology and cardiovascular diseases.

Dr. Helmy was a recipient of the Department of Medicine Distinguished Teaching Award in 1997, the Trustees Teaching Award in 1998, 2000, and 2005, the General Internal Medicine/Geriatrics Division Outstanding Teacher Award in 2001, the Outstanding Professor in Clinical Sciences Award in 2003 and 2004, the School of Medicine Teaching Award in 2005, and the Outstanding Educator Award in 1999, 2003, and 2006, which is given by the departing class of IU School of Medicine senior residents to the faculty member who has contributed most significantly to their education during their residency. He was also a recipient of the 2007 Presidential Award at the Indiana University.

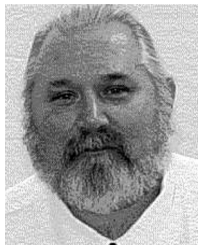

Michael M. Holdmann received the B.S.E.E. and the M.S.E.E. degrees from the Indiana University-Purdue University (IU), Indianapolis, IN, in 1990 and 1997, respectively.

He is a Professional Engineer registered in the state of Indiana. His research interests include automation, robotics, applied superconductivity, and medical electronics.

Maher E. Rizkalla (SM'95) received the B.S. degree from Assiut University, Assuit, Egypt, in 1975, the M.S. degree from Cairo University, Cairo, Egypt, in 1980, and the Ph.D. degree from Case Western Reserve University (CWRU), Cleveland, OH, in 1985, all in electrical engineering.

In September 1986, he joined the Department of Electrical and Computer Engineering, Indiana University Purdue University (IUPUI), Indianapolis, IN, where he is currently a Professor and Associate Chair. From January 1985 to September 1986, he was a Visiting Scientist with the Solid State Group, Argonne National Laboratory, Argonne, IL, while he was a Visiting Assistant Professor with Purdue University Calumet (PUC), Hammond, IN. He has published over 120 papers in journals and conference proceedings.

Dr. Rizkalla is the P.I. of an NSF grant, two FIPSE grants, and a Co-P.I. of a number of industrial research grants. He is a professional engineer registered in the State of Indiana.